ChemComm

Accepted Manuscript

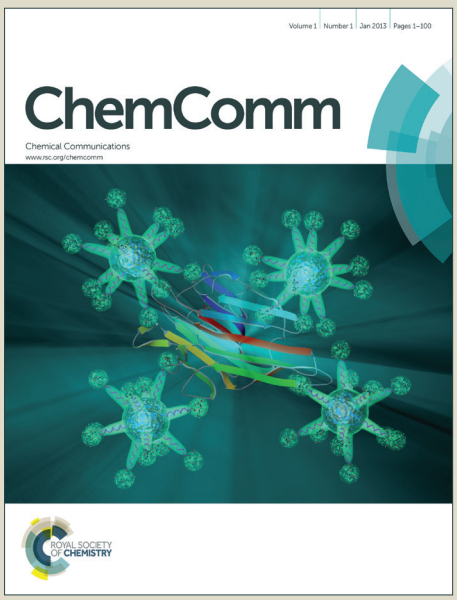

ROYAL SOCIETY OF CHEMISTRY

www.rsc.org/chemcomm

ChemComm

RSCPublishing

COMMUNICATION

N-doped carbon spheres with hierarchical micropore-nanosheet networks for high performance supercapacitors

Cite this: DOI: 10.1039/x0xx00000x

Shoupei Wang, Jianan Zhang, Pei Shang, Yuanyuan Li, Zhimin Chen, Qun Xu**

Received 00th June 2014,
Accepted 00th June 2014

DOI: 10.1039/x0xx00000x

www.rsc.org/

N-doped carbon spheres with hierarchical micropore-nanosheet networks were facilely fabricated by one-step carbonization and activation process of N containing polymer spheres by KOH. With the synergy effect of the multiple structures, HPSCSs exhibit a very high specific capacitance of 407.9 F g^{-1} at 1 mV s^{-1} (even 1.2 times than that of porous carbon spheres) and robust cycling stability for supercapacitors.

Carbon materials have recently attracted widespread attention concerning their applications in energy storage systems such as double-layer electrochemical capacitors (ECs) and Li-ion batteries, [1-3] owing to the following important properties: (a) their highly porous structures, (b) good chemical stability and (c) high electronic conductivity.[4-8] These properties have enabled these materials the preferred excellent candidate for manufactures on fabricating electrodes for EC devices. More specifically, porous carbons with high surface areas and a porosity established with microporous varying in ~0.7-1 nm constitute the best options for ECs because they exhibit the largest specific capacitance values.[9] But the specific capacitance decrease dramatically with increasing the discharging rate due to the increasing mass-transfer resistance through the small-sized channels. In order to overcome this issue, it is crucial to improve the ions-diffusion efficiency and election-transport kinetics. Two strategies have been adopted for this purpose. Recently, many researches force on the fabrication of carbons with hierarchical porous structures that combine macropores, mesopores, and micropores.[10] The multimodal porous tissue is more suitable for high performance ECs, because the macropores act as ion-buffering reservoirs and the mesoporous offer channels for the rapid mass transport.[11,12] However, the maximum specific capacitance is still low, probably owing to the relatively poor electronic conductivity of porous carbon materials in most cases. As an interesting alternative, 2-dimensional (2D) planner carbon materials, e.g. graphene, are highlighted by their high conductivity and large surface area. Unfortunately, the highest theoretical capacitance for graphene is still far from realization probably due to their one-fold structural type that lacks abundant active surface (because of their self-restacking) and ordered tunnel for mass diffusion.

Recent studies revealed that the rational combination of porous and nanosheet structures gives a new opportunity to promote the properties of carbon materials. Prominent examples include synthesis of interconnected carbon nanosheet made up of porous structures with specific capacitance of 113-142 F g^{-1},[11] the intercalation of mesoporous carbon spheres into the reduced graphene oxide layers with specific capacitance of 171 F g^{-1},[13] and coating the graphene with microporous carbon layer with specific capacitance of 103 F g^{-1}.[14] Despite their great potentials in ECs, the development of these materials is based on the 2D structured carbon, which probably limited the readily direct diffusion of electrolyte ions and electrons compared to the 3D structure, and thus leading to relatively poor performance. Undoubtedly, it will be of great significance to develop carbon materials with multiple structures consist of hierarchical pores and nanosheet, and also a 3D large interconnected network, which can afford efficient charge and mass exchange and low internal resistance during the charging/discharging capacitor process.

Previous studies have revealed that doping nitrogen into carbon frameworks can enhance their capacitance performance, but the resulted carbon electrodes can hardly achieve both high-capacitance and high-rate capability.[15,16] Herein, we describe a facile carbonization and activation process to prepare N-doped carbon spheres with hierarchical micropore-nanosheet networks (HPSCSs), indicating the coexistence of multiple porous and nanosheet structures in HPSCSs. The synergistic effect of the multiple structures in HPSCSs is highly important for enhancing electrochemical performance. As a result, the HPSCSs demonstrate a ultrahigh specific capacitance of 407.9 F g^{-1} at 1 mV s^{-1}, which is about 1.2 and 4.0 times than that of the porous carbon spheres (PCSs) and non-activated carbon spheres (CSs). And also, they exhibit high rate capability (71.1% capacitance retention at 100 mV s^{-1}) and extremely excellent cycling performance (99.0% capacitance retention even after 6000 cycles at 10 A g^{-1}).

HPSCSs were synthesized by one-step carbonization and activation process of nitrogen containing polymer spheres (NPSs) using KOH as chemical reagent. Briefly, uniformly resorcinol-melamine-formaldehyde spheres were first prepared in an ethanol-water-ammonia system under hydrothermal treatment. The scan electron microscopy (SEM) and transmission electron microscopy (TEM) images of the NPSs are shown in **Fig. 1a&b.** The well-defined NPSs show a uniform diameter of about 500-550 nm with smooth surfaces and nonporous structure. Then, the heat-treatment

of a mixture of the NPSs and KOH (mass ratio is 1:2) under an inert atmosphere directly leads to the formation of HPSCSs. Commonly, the activation of active carbon undergoes by etching the carbon framework of pre-calcination chars. But this time-consuming protocol often crudely destroys the morphology and collapses the structures. In our method, the activation occurred during the pyrolysis and gasification of polymer. The heat generate in this process probably accelerate the production of potassium composites, which have played a crucial role in the development of the microporous network. Meanwhile, the metallic K (produced *via* the reaction of K_2O by carbon) is intercalated between the expanded carbon lattices, resulting in exfoliation of carbon layer to a certain extent.[17, 18] The morphology and microstructure of the carbon samples were examined by SEM and TEM. **Fig. 1c** shows that as-prepared HPSCSs display a relatively spherical morphology with a remarkable rougher external surface and a diameter of 250-280 nm, smaller than their original NPSs, which was probably caused by peeling off the outer carbon layer during activation and particle shrinkage.[19] **Fig. 1d-f** give the TEM images of HPSCSs at different magnifications. It is found that HPSCSs demonstrate an interesting 3D architecture of random carbon nanosheets connected with honeycombed carbon structure. Particularly, the high-resolution TEM (HRTEM, **Fig. S3**) image reveals that the individual carbon layer possess both wormlike porous structure and crystalline regions on the edges. The crystalline regions are formed by 3-5 parallel fringes with an interlayer d-spacing of 0.38 nm, indicating a good graphitic structure of HPSCSs.

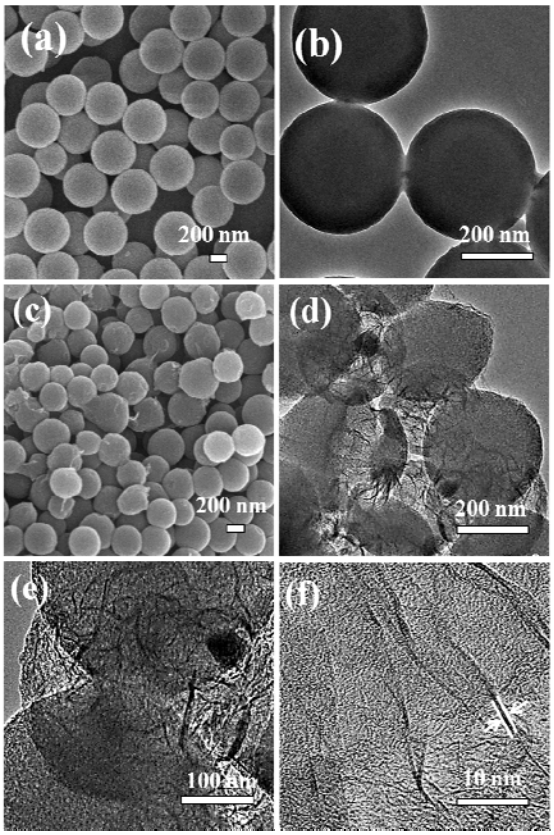

Fig. 1 SEM images of (a) NPSs, (c) HPSCSs. TEM images of (b) NPSs, (d-f) HPSCSs at different magnifications.

As a comparison, the PCSs were also obtained *via* the above synthetic strategy but using K_2CO_3 as chemical reagent. It is interestingly found that the uniform PCSs possess homogenous porous structure but without any nanosheet region (**Fig. S1**), which might be caused by the relatively weak basic activation reaction between K_2CO_3 and carbon. The non-activated CSs (**Fig. S2)** were further prepared as a control to demonstrate the distinct electrochemical performance of HPSCSs.

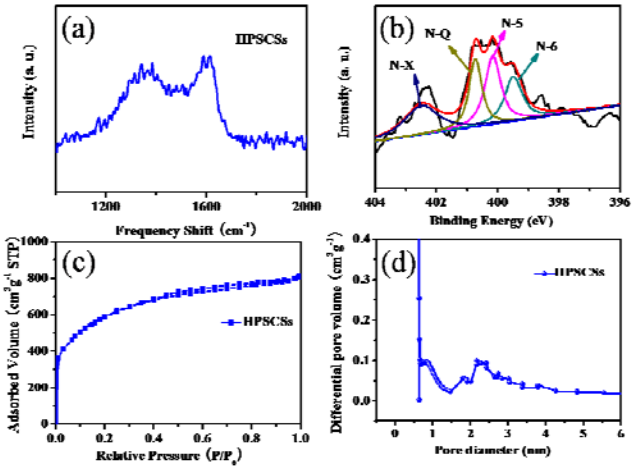

Fig. 2 (a) Raman spectrum, (b) N1s spectrum of HPSCSs, (c) N2 adsorption-desorption isotherms and (d) pore size distribution (estimated by the adsorption isotherm) of HPSCSs.

To further understanding the property of HPSCSs, the structural characterizations of HPSCSs were monitored by Raman, XPS, BET measurements. As shown in **Fig. 2a**, Raman spectrum of HCNCs displays the higher ratio of I_G/I_D (I_D and I_G are related to the A_{1g} vibration mode of the disordered carbon (D-bond) and the E_{2g} vibration mode of the ordered graphitic carbon (G-bond)) than that of reduced graphene oxide.[20,21] The XRD pattern of HPSCSs (**Fig. S4**) exhibit two obvious peaks at 25° and 43°, assigned to (002) and (100) planes of hexagonal carbon material, respectively. The results from the Raman spectrum, XRD pattern, and HRTEM image reveal that the nanosheet in HPSCSs features graphitic order with crystalline domains, promising good conductivity. **Fig. 2b** depicts the high resolution X-ray photoelectron spectroscopy (XPS) of N 1s for HPSCSs. By using a Gaussian fitting method, the N 1s spectrum could be curve-fitted into four-type peaks, which are correlated to different electronic states of nitrogen functional groups: pyridinic (N-6, 398.6 eV), pyrrolic groups (N-5, 400.9 eV), quaternary nitrogen (N-Q, 402 eV), and pyridine N-oxide (N-X, 403 eV), respectively.[22] The existing studies reveal that the pseudocapacitive interactions take place on negatively charged N-5 and N-6, while the positive charge on N-Q and N-X helped in electron transfer through the carbon, enhancing the conductivity of carbon materials.[15] Moreover, the doping of nitrogen in HPSCSs is 1.585 wt% (monitored by XPS).

Nitrogen adsorption-desorption isotherms and the pore size distribution (PSD) curves of the HPSCSs are shown in **Fig. 2c&d**. The isotherm exhibits a typical characteristics of type I curves with an almost horizontal plateau at higher relative pressures and the absence of hysteresis, indicating highly microporous materials. Some of the isotherms show an increasing slope for values P/P_0 >0.9, indicating the development of wider pores.[23,24] The BET surface area, micropore surface area, and total pore volume of the porous carbons are summarized in **Table S1** for easy comparison. The BET surface areas of HPSCSs and PCSs are 2118.0, 2779.0 m^2g^{-1}, respectively, remarkable larger than that of 580.4 m^2g^{-1} (**Fig. S5**). This is mainly owing to the creation of a high volume of fine micropores (pore<2

nm) during the high temperature activation process. The PSD curve of HPSCSs from adsorption data shows sharp peaks at 0.8, 1.0, and 2.3 nm, indicating the hierarchical micropores and mesopores in the sample, in good agreement with the observation results obtained by TEM. Such a hierarchical porous nanostructure offers easy access of electrolyte to the surface of carbons to form electric double layers.

The unique structure of HPSCSs inspired us to evaluate their electrochemical performance for supercapacitor. Cyclic voltammetry (CV), galvanostatic charge-discharge, and electrochemical impedance spectroscopy [25] were measured with a three-electrode system in a 6 M KOH aqueous electrolyte (**Fig. 3**). As shown in **Fig. 3a,** CV curves of HPSCSs at different current shows a capacitive behavior with roughly rectangular-like shapes and reversible humps**,** attributed to the combination of electric double-layer capacitance (EDLC) and pseudocapacitive reaction. It should be noticed that the rectangular shape of HPSCSs maintains even at a high potential scan rate of 400 mV s^{-1} (**Fig. S6**). HPSCSs also exhibit good rate capability of 71.1% and 61.6 % capacitance retention at 100 mV s^{-1} and 200 mV s^{-1} compared to the capacitance at 1 mV s^{-1}, respectively, which indicates the pure EDLC behaviour and the rapid formation of the double-layer even at high rates.

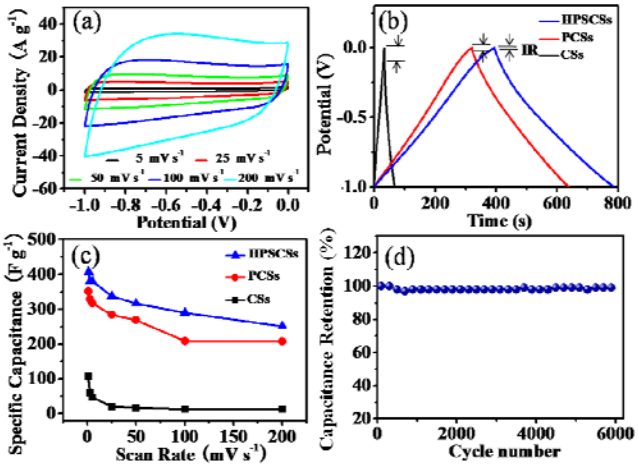

Fig. 3 (a) CVs curses of HPSCSs electrode at different scan rates. (b) galvanostatic charge-discharge curves of HPSCSs, PCSs and CSs at a current density of 0.5 A g^{-1}. (c) Specific capacitances of HPSCSs, PCSs and CSs electrodes at different scan rates. (d) Capacitance retention versus the cycle number of HPSCSs measured at 10 A g^{-1}.

To verify the synergetic effect between hierarchical porous structure and nanosheet in the network of HPSCSs, we compared the capacitance properties of HPSCSs, PCSs and CSs. Fig. 3b shows the galvanostatic charge-dicharge profiles of all samples. The typical charge-discharge curve of HPSCSs is nearly linear and symmetric with a gradual slop change, indicating the ideal capacitor behaviour of HPSCSs. Significantly, at a given current density of 0.5 A g^{-1}, the IR drop (resistance drop) of HPSCSs (0.22 V) is remarkable smaller than that of PCSs (0.31 V) and CSs (0.51 V). It is generally accepted that the IR drop is related to the electrical conductivity and porous texture (including the connectivity, size distribution, shape of pores) of the electrode.[10] Therefore, the lower IR drop of HPSCSs than that of PCSs and CSs can be attributed to the synergy of rapid mass transport pathway of hierarchical porous structure and high-conductivity of nanosheet. In the case of PCSs, the lack of very short inner-pore transport pathway will inevitably lead to a significant ionic diffusiona loss contribution to the IR drop.[26] This point is further conformed by the EIS of the samples (**Fig. S6b**). Typically, HPSCSs exhibit lower resistance (0.67 Ω) than that of PCSs (0.92 Ω), indicating the higher conductivity of HPSCSs. As a result, HPSCSs shows the highest specific capacitance of 407.9 F g^{-1}, which is about 1.2 and 4.0 times than that of PCSs (351.1 F g^{-1}) and CSs (107.0 F g^{-1}), even if the BET surface area of HPSCSs is smaller than that of PCSs (**Fig. S5** and **Table S1**). **Fig. 3d&S6c** present the cycling performance of HPSCSs at current density of 10 A g^{-1}. HPSCSs exhibits a very a stable capacitance (99.0% of the original capacitance) after 6000 cycles of charging and discharging, indeed indicating its long-term electrochemical stability. This is further conformed by the inconspicuous change between charging-discharging curves of first and 6000th cycle. According to **Table S2,** HPSCSs exhibit the best performance for supercapacitor than the state-of-the-art carbon materials ever reported (**Table S2**). Taking into account of their high specific capacitance and the very robust electrochemical stability, HPSCSs present promise as the electrode candidate for supercapacitor.

In summary, HPSCSs with hierarchical porous-nanosheet nanonetworks were simply fabricated by one-step carbonization and activation process of resorcinol-melamine-formaldehyde spheres by KOH. Through combining multilevel porosity, partially graphitic nanosheet, and N heteratomic functionalities, the as-obtained HPSCSs manifest a significant improved specific capacitance compared to PCSs and CSs, giving a reversible specific capacitance of 407.9 F g^{-1} and 99.0% capacitive retention after 6000 cycles. We believe such structure integration is available for a lot of applications, such as catalysis, fuel cell, and lithium ion batteries.

This work was financially supported by the National Natural Science Foundation of China (Nos. 21101141 and 51173170), the financial support from the Program for New Century Excellent Talents in Universities (NCET), and the Open Project Foundation of State Key Laboratory of Inorganic Synthesis and Preparation Chemistry of Jilin University (2012-13).

Notes and references

College of Material Science and Engineering, Zhengzhou University, Zhengzhou 450001, R. P. China.

E-mail: zjn@zzu.edu.cn (Jianan Zhang) and qunxu@zzu.edu.cn (Qun Xu)

† Electronic Supplementary Information [27] available: See DOI: 10.1039/c000000x/

1. Y. Cao, M. Zhu, P. Li, R. Zhang, X. Li, Q. Gong, K. Wang, M. Zhong, D. Wu and F. Lin, *Phys. Chem. Chem. Phys.*, 2013, **15**, 19550-19556.
2. X. Zang, Q. Chen, P. Li, Y. He, X. Li, M. Zhu, X. Li, K. Wang, M. Zhong and D. Wu, *Small*, 2014, **13**, 2583-2588.
3. X. Li, X. Zang, Z. Li, X. Li, P. Li, P. Sun, X. Lee, R. Zhang, Z. Huang and K. Wang, *Adv. Funct. Mater.*, 2013, **23**, 4862-4869.
4. C. Liang, Z. Li and S. Dai, *Angew. Chem. Int. Ed.*, 2008, **47**, 3696-3717.
5. C. Vix-Guterl, E. Frackowiak, K. Jurewicz, M. Friebe, J. Parmentier and F. Béguin, *Carbon*, 2005, **43**, 1293-1302.
6. J. Lee, J. Kim and T. Hyeon, *Adv. Mater.*, 2006, **18**, 2073-2094.
7. J. Wang and S. Kaskel, *J. Mater. Chem.*, 2012, **22**, 23710-23715.
8. W. Xiong, M. Liu, L. Gan, Y. Lv, Y. Li, L. Yang, Z. Xu, Z. Hao, H. Liu and L. Chen, *J. Power Sources*, 2011, **196**, 10461-10464.
9. J. Chmiola, G. Yushin, Y. Gogotsi, C. Portet, P. Simon and P. L. Taberna, *Science*, 2006, **313**, 1760-1763.
10. D. W. Wang, F. Li, M. Liu, G. Q. Lu and H. M. Cheng, *Angew. Chem. Int. Ed.*, 2008, **47**, 373-376.
11. M. Sevilla and A. B. Fuertes, *ACS Nano*, 2014, **8**, 5069-5078.
12. D. Bhattacharjya, M. Kim, T. Bae and J. Yu, *J. Power Sources*, 2013, **244**, 799-805.
13. Z. Lei, N. Christov and X. S. Zhao, *Energy Environ. Sci.*, 2011, **4**, 1866-1873.
14. X. C. Guo and M. C. Li, *Energy Environ. Sci.*, 2011, **4**, 4504-4507.
15. D. Hulicova-Jurcakova, M. Kodama, S. Shiraishi, H. Hatori, Z. H. Zhu and G. Q. Lu, *Adv. Funct. Mater.*, 2009, **19**, 1800-1809.
16. H. Chen, F. Sun, J. Wang, W. Li, W. Qiao, L. Ling and D. Long, *J. Phys. Chem. C*, 2013, **117**, 8318-8328.
17. J. Wang and S. Kaskel, *J. Mater. Chem.*, 2012, **22**, 23710-23725.

18. J. Romanos, M. Beckner, T. Rash, L. Firlej, B. Kuchta, P. Yu, G. Suppes, C. Wexler and P. Pfeifer, *Nanotechnology*, 2012, **23**, 015401-015408.
19. T. Liou, Horng, *Chem. Eng. J.*, 2010, **158**, 129-142.
20. J. Zhang, K. Wang, S. Guo, S. Wang, Z. Liang, Z. Chen, J. Fu and Q. Xu, *ACS Appl. Mater. Interfaces*, 2014, **6**, 2192-2198.
21. Y. Guo, S. Guo, J. Ren, Y. Zhai, S. Dong and E. Wang, *ACS Nano*, 2010, **4**, 4001-4010.
22. D. Hulicova-Jurcakova, M. Seredych, G. Q. Lu and T. J. Bandosz, *Adv. Funct. Mater.*, 2009, **19**, 438-447.
23. F. Su, C. K. Poh, J. S. Chen, G. Xu, D. Wang, Q. Li, J. Lin and X. W. Lou, *Energy Environ. Sci.*, 2011, **4**, 717-724.
24. J. Zhang, S. Guo, J. Wei, Q. Xu, W. Yan, J. Fu, S. Wang, M. Cao and Z. Chen, *Chem. Eur. J.*, 2013, **19**, 16087-16092.
25. H. Shi, W. Li, L. Zhong and C. Xu, *Industrial & Engineering Chemistry Research*, 2013.
26. E. Frackowiak, *Phys. Chem. Chem. Phys.*, 2007, **9**, 1774-1785.
27. E. Seo, J. Kim, Y. Hong, Y. S. Kim, D. Lee and B.-S. Kim, *J. Phys. Chem. C*, 2013, **117**, 11686-11693.

